

Dual Band Integrated Wideband Multi Resonating Patch Antenna for C–Band and Ku–Band Applications

Karunesh Srivastava, Sweta Singh, Aditya Kumar Singh and Rajeev Singh

Abstract—A wideband antenna with dual band characteristic at 5.33/14.3GHz with resonating frequencies for wireless applications is presented. The strategy of the design is to introduce multiband in antenna band. Bandwidth of the antenna increases by embedding annular ring on the radiating patch and four bands are achieved by introducing coupling gap between the patches. Surface current distribution is analyzed at different resonating frequencies for understanding the radiation mechanism and effect of annular ring. The antenna parameters such as return loss, radiation pattern, gain, VSWR and group delay are discussed. The impedance bandwidth of the proposed dual band antenna at lower resonant frequency is 12.7% (simulated) and 9.8 % (measured) whereas at upper resonant frequency is 15.3 % (simulated) and 13.97 % (measured).

Keywords—Micro-strip antenna, Dual-band, wideband, C-band, Ku-band and HFSS.

I. INTRODUCTION

SINCE the inception of the radio waves, wireless communication has technologically matured and has seen applications in satellite and radar communication which in turn has increased the necessity of wideband, multiband and antenna's with very small dimensions [1,2].

In wireless applications different antennas have been reported for different bands like multi band [3-7], wideband [8-10] and ultra wide band [11-15]. Numerous antenna array techniques for Ku (Kurtz-under band) band satellite, TV reception [16-18] and for C-band applications such as rectangular patch antenna arrays [17], stacked printed antennas array [18], circularly polarized square slot array antenna [19], planar micro strip array antennas [20] have been reported. A micro-strip patch feed reflector antenna has been reported in [21] for C-band applications.

Various micro-strip antennas operating in Ku band have been reported [6,13-23]. Several articles reported earlier cover single band, dual band and multi band antenna with applications of C-band [24-27], Ku-band[6,13-23]. However, any antenna design which covers both C and Ku bands is not reported. To design an antenna which can cover C-band and Ku-bands both, a trade-off between the physical parameters and the electrical parameters is required. We propose a new design of micro strip patch antenna which covers both C-band and Ku-band on a single patch. The antenna has been designed and simulated using Ansoft HFSS v13 and the prototype has been fabricated in lab for experimental verification.

II. ANTENNA DESIGN AND SYNTHESIS

As outlined in the introduction the antenna design is intended to cover C and Ku bands both, therefore, the parametric analysis of different shapes, coupling gaps, shorting pin positions and radius of annular ring have been performed in order to arrive at the best geometrical configuration with optimized antenna parameters. Four different antenna structures shown in figure 1 have been designed and simulated. The geometrical top view and the fabricated top view of the proposed micro-strip patch antenna are shown in Fig.1 (d) and Fig.2 respectively. The patch of proposed antenna is divided into two parts, one is fed patch and other is parasitic patch. The patch closed to the fed /driven patch gets energy through suitable radiating coupling is known as parasitic patch.

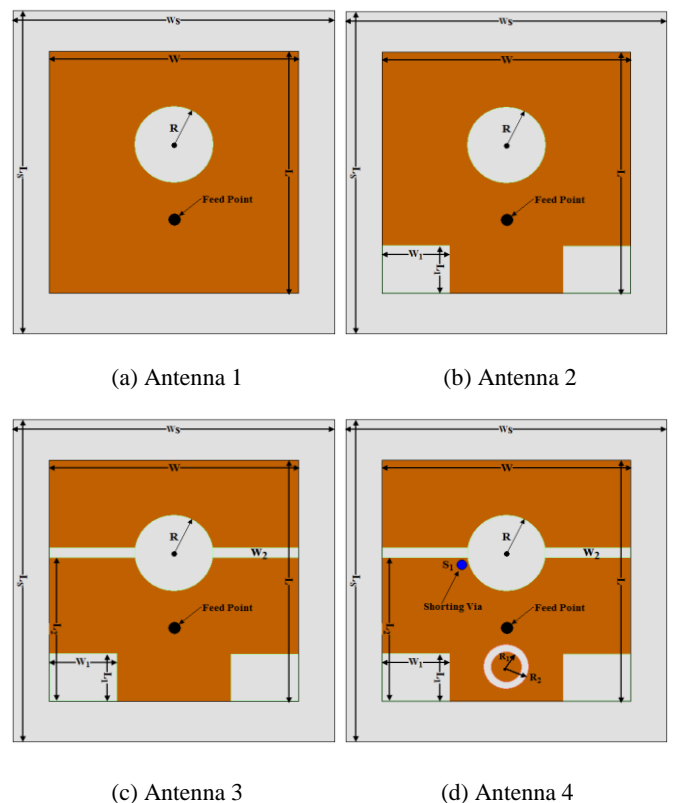


Fig. 1. Top view of the geometrical structure of the proposed antenna

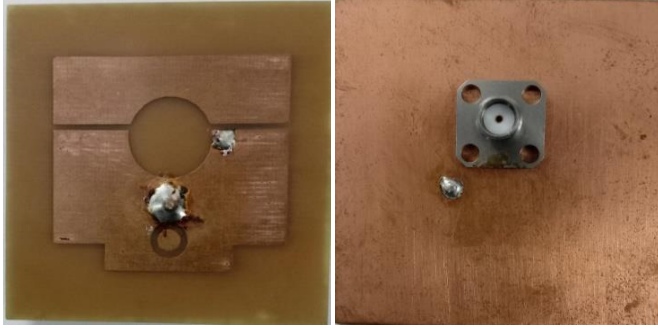


Fig.2. Top & back view of the fabricated prototype antenna

TABLE I
GEOMETRICAL SPECIFICATIONS OF THE PROPOSED ANTENNA

Geometrical Parameters	Parameter Values
Dimension of ground ($L_s \times W_s$)	50mm \times 50mm
Thickness of dielectric material/dielectric constant	1.6 mm/4.4
Dimension of patch ($L \times W$)	31mm \times 33mm
Dimension of rectangular notch at lower corner of patch ($L_1 \times W_1$)	4mm \times 7.5mm
Dimension of rectangular slot ($W_2 \times W$)	1mm \times 36mm
Radius of circular cut in rectangular patch (R)	6mm
Radius of the annular slot ($R_2 - R_1$)	1mm
Gap between patches (W_1)	1mm
Reference point	(0,0) mm
Shorting pin position	(-4,-7) mm
Radius of Shorting pin	1mm
Feed point	(8,0) mm

II A. PARAMETRIC ANALYSIS OF SHAPE, COUPLING GAP, SHORTING PIN POSITION AND RADIUS OF ANNULAR RING

A. Parametric Analysis of Shape

Radiating patch of Antenna-1 and Antenna-2 are rectangular shaped and a circular slot is being cut out from Antenna-1, and further two rectangular notches (4 \times 7.5) mm are removed from the lower part of the radiating patch of Antenna-1 to form Antenna-2. Geometry of Antenna-3 is obtained by introducing a slot of (1 \times 36) mm along x-axis of the radiating patch thus creating an electromagnetic coupling gap. Antenna-4 is the proposed antenna where as additional annular ring is loaded along with a shorting pin at position (-4,-7) mm near the left side of the main circular slot. The radiating patch of the wideband antenna structure consists of circular slot and a linear gap between patches, annular slot and finally inserting a shorting pin. Circular slot and the linear gap between patches provide a gap coupled structure for Antenna -4 (cf. Fig.1 (d)). Fig. 1(d) shows the geometry of the proposed antenna and Table I shows the geometrical specifications of the proposed antenna. Antenna is excited by coaxial feed line with radius of 1 mm to achieve 50 Ω impedance match. The purpose of introducing a slot or notch is to reduce overall area of the patch. It also changes the inductive and capacitive behavior of the distributed elements and the lumped elements.

It is observed (cf. Fig 3(a) & Fig. 3(b)) that Antenna-1&2 starts resonating only after 7.27 GHz with sufficient return loss, therefore; these two antennas are not useful for desired C band applications. Rectangular notch at lower patch improves the return loss of antenna whereas introduction of slot increases the resonating bands of antenna. Shorting pin is used for enhancing the gain of antenna. Annular ring is used for increasing the band width towards higher band. Embedding ring on the radiating patch results into the change in the surface current distributions. Calculated impedance bandwidths of proposed dual band antenna are 12.7%

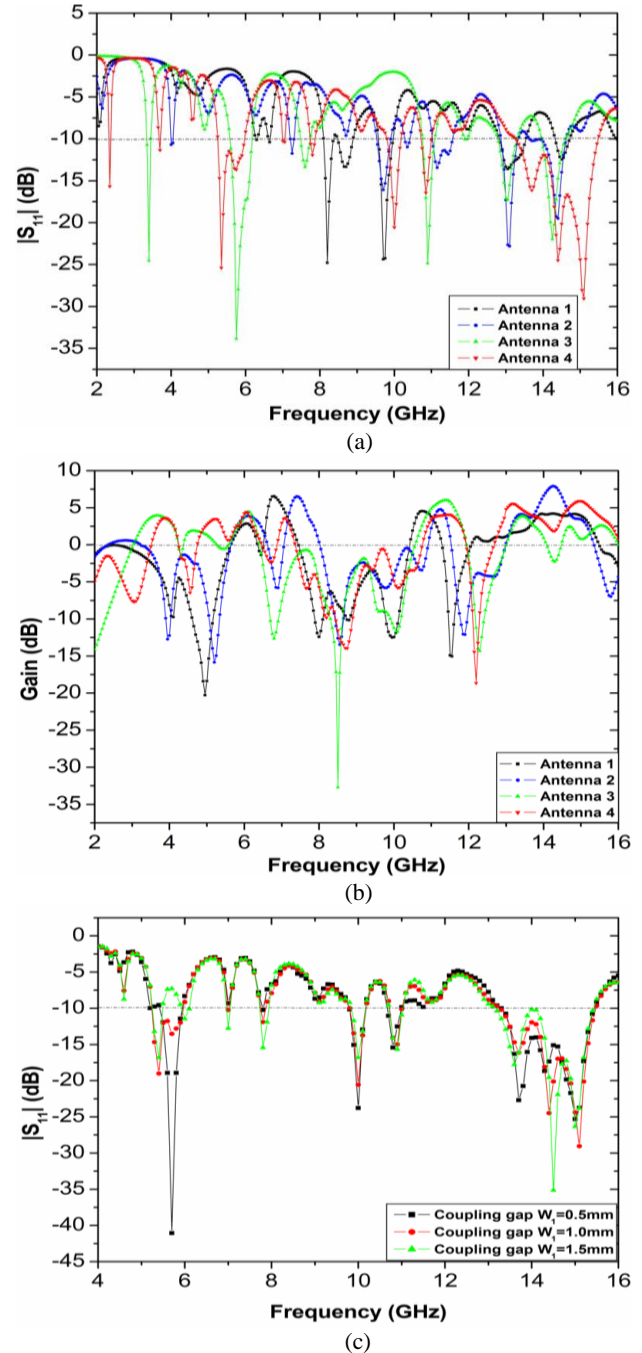


Fig.3 (a) Parametric analysis of shape of return loss as function of frequency,(b) Parametric analysis of shape of gain as function of frequency,(c) Parametric analysis of coupling gap W_1 of simulated return loss as function of frequency.

(simulated) and 9.8 % (measured) for the lower band at central frequency. Similarly for the band at higher central frequency the calculated values of impedance bandwidth are 15.5% (simulated) and 13.97% (measured). Minor deviation is observed between simulated and measured result.

B. Parametric Analysis of Coupling Gap

Effect of coupling gap W_1 is depicted in Fig. 3(c) by means of return loss versus frequency variation. At the lower operating band (5.26-5.94GHz), variation in coupling gap ($W_1=0.5\text{mm}$ to 1.5mm in steps of 0.5mm) results into a shift of band for 0.5mm and 1.5mm gaps (cf. Fig. 3(c)). At the gap of 0.5mm, the lower starting frequency is observed at 5.40GHz and at the gap of 1.5mm the starting frequency is 5.24GHz but the band ends at 5.49GHz reducing the overall bandwidth. From Fig. 3(c) we observe; the starting frequency at 5.24GHz and end frequency of band at 5.94GHz which gives a better bandwidth. At frequency band (13.25-15.47GHz) only a marginal shift towards lower frequency is observed (cf. Fig.3b) due to variation in gap coupling. However, for gap value of 1.5mm we observe that at 14.05GHz, the return loss value just touches -10dB emission point which is not desirable. In view of the above discussion, $W_1=1\text{mm}$ is chosen as the optimum coupling gap for the proposed antenna.

C. Parametric Analysis of Shorting Pin Position

A simulated gain of the proposed antenna without shorting pin, and with shorting pin at different positions is illustrated in Fig.4 (a). The shorting pin was rotated along with the left half of the circumference of the circular slot of fed patch i.e. from position (3, 0) to (-4,-7). On observing the result, we can conclude that the antenna without shorting pin and with shorting pin at other positions except (-4,-7) do not exhibit better gain in the operating bands viz. 5.26-5.94 GHz and 13.22-15.50 GHz than the proposed position (-4,-7). From Fig.4(a) we observe maximum gain values of 0.41dB, 0.66dB, 0.28dB and 3.6dB for without shorting pin and at (3,0), (2,-4) and (-4,-7) respectively in the frequency band (5.26-5.94GHz). However, the gain values become negative from 5.32GHz for all positions and without shorting pin except the proposed position i.e. (-4,-7) in the operating band (5.26-5.94GHz). For the second operating band (13.22-15.50GHz) we observe maximum gain values of 2.6dB (without shorting pin), 2.4dB (at 3,0), 2.1dB(at 2,-4) and 5.6dB (at -4,-7) at the band starting position (13.22GHz). However, we do not observe gain from 13.95GHz to 14.5GHz for any position including without shorting pin, except for the proposed position (-4,-7).The maximum gain achieved by the antenna configuration without shorting pin, at positions (3, 0),(2,-4) is 4.55dB, 3.26dB and 3.10dB respectively, whereas we achieve 6.0dB for the proposed position (-4,-7). On the basis of the above discussion we propose to choose (-4,-7) as the best co-ordinate position for posting the shorting pin.

D. Parametric Analysis of Radius of Annular Ring

Parametric analysis of radius of annular ring is performed for investigating the frequency domain behavior of $|S_{11}|$ of the proposed structure.

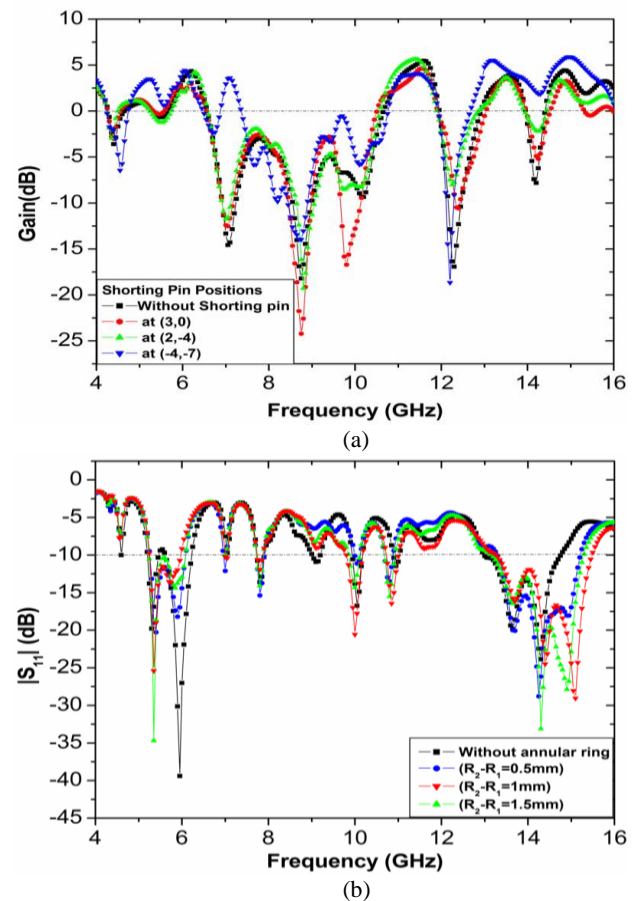


Fig.4. (a) Parametric analysis of shorting pin position by analyzing gain as function of frequency,(b) Parametric analysis of radius of annular ring by analyzing simulated return loss as function of frequency

Annular ring consists of gap capacitance C_g and plate capacitance C_p of the micro-strip line and it can be represented as two parallel micro-strip lines [7]. The equivalent circuit for annular ring with patch can be expressed as the parallel combination of R, L, C (for inner ring) and G, L, C (or outer ring) [7]. From Fig. 4(b) it is observed that the variation in radius (R_2-R_1) of annular ring (in steps of 0.5mm) hardly affects the starting point (5.2 GHz) of the lower band but for (R_2-R_1) of 0.5mm and 1.5mm the band ends at 6.08 GHz as compared to proposed (R_2-R_1) of 1.0mm which ends at 5.94 GHz. Further, the antenna without annular ring shows two distinct bands one from 5.18 to 5.47 GHz and second from 5.62 to 6.22 GHz. The variation of (R_2-R_1) is more pronounced at higher frequency band. We observe that band for antenna without annular ring is from 12.98 GHz to 14.76 GHz, for (R_2-R_1) = 0.5mm is 13.30 GHz to 15.22 GHz, for (R_2-R_1) = 1.0 mm is 13.22 GHz to 15.50 GHz and for (R_2-R_1) = 1.5mm is 13.11 GHz to 15.28 GHz. We observe a shift in frequency as the (R_2-R_1) is changed but due to the fact that the highest bandwidth with maximum return loss (-28.98dB) is observed in case of (R_2-R_1) = 1.0mm, therefore, the same is chosen as the optimum (R_2-R_1) of the annular ring for the proposed antenna.

III. RESULTS AND DISCUSSION

Geometry of the proposed antenna is shown in Fig.1 (d) and top and bottom views of fabricated antenna are shown in Fig.2. In the present work a rectangular shaped patch having circular slot on patch and two rectangular notches at lower side (geometries given in Table I) is used. The proposed antenna is fabricated and experimentally tested to verify the simulated antenna parameters. Simulation of designed antenna has been performed using Ansoft HFSS version 13 and the simulated results have been verified experimentally. The behavior of antenna is observed in terms of return loss, gain, radiation pattern, current distribution and voltage standing wave ratio.

Fig. 5(a) shows simulated return loss of antenna-4 (proposed antenna) and it is clear that Antenna-4 resonates at four frequencies. The observed simulated (measured) resonant frequencies are 5.33 GHz (5.4 GHz), 10GHz (10GHz), 10.85 GHz (10.9GHz) and 14.3 GHz (14.31GHz). The difference between measured and simulated resonant frequencies is within the permissible limit and the minor deviation arises due to stray, fringe capacitances and fabrication errors. Simulated (measured) impedance bandwidths at -10 dB are 650MHz (550MHz), 300MHz(250MHz), 300MHz(200MHz) and 2.15GHz(2GHz) which is calculated from Fig.5(a). The HFSS tool uses finite elements method to calculate and predict the resonant frequency as well as the impedance bandwidth but the difference between measured and simulated bandwidth arises due to several approximations and assumptions in calculation of fringe capacitance, extension length, loss tangent and effective dielectric constant for the chosen dimensions of the patch[28]. The simulated (measured) result cover the frequency band from 5.24-5.95 GHz (5.35-5.9 GHz) and 13.25-15.47 GHz (13.35-15.35 GHz). The measured and simulated results exhibit that it covers C, X and Ku- band of EM spectrum. However, simulated gain of the proposed antenna is not meeting the expectation of return loss of proposed antenna (cf. Fig.5 (b)).

Therefore, it can be inferred that antenna is suitable for C-band and Ku-band but is resonating at four frequencies. Simulated peak value of gain for C-band (commercial telecommunication via satellite) and Ku-band (used for fixed satellite broadcast services) is 3.73dB and 5.89dB.

In Fig. 5(a) we observe "ringing resonant frequencies" [7] in the operating band of 13.22-15.50 GHz. As discussed in [7], the gain performance in the specified band becomes unstable and it varies considerably during the specified band. From Fig. 4(a) we observe the gain (values) at 13.22 GHz (5.48dB), 13.66 GHz (3.97dB), 14.03 GHz (3.07dB), 14.40GHz (2.70dB), 14.62 GHz (4.5dB), 15.09 GHz (5.8dB) and 15.50 GHz (3.89dB). The "ringing resonant frequencies" are occurring at 13.66 GHz, 14.40 GHz and 15.09 GHz and upon observing Fig. 4(a), we can conclude that the gain values at these "ringing resonant frequencies" are 3.97dB, 2.70dB and 5.8dB. It is interesting to note at 15.09 GHz, we observe

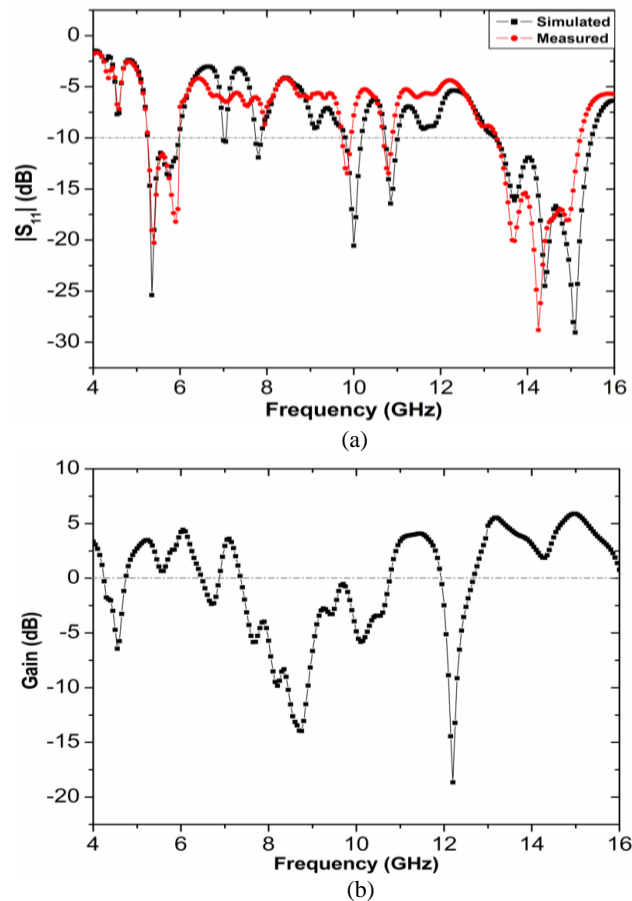


Fig.5. (a) Simulated and measured return loss as function of frequency of the proposed antenna, (b) Simulated gain as function of frequency of the proposed antenna

maximum return loss (-28.98dB) amongst the three "ringing resonant frequencies" which may be the reason of maximum observed gain. The lowest peak of third ringing resonant frequency starts from 15.09 GHz and ends up at 15.50 GHz, where we observe a decrease in gain from 5.8dB to 3.89dB. From the above discussion it can be safely concluded that when the multiple resonating peaks (ringing resonant frequencies) are observed in a single band then the overall gain varies during the entire band and it does not remain stable.

Measured and simulated VSWR as a function of frequency are shown in Fig. 6(a) which is below 2 in all the cases and confirms the results of return loss behavior and is suggestive of good impedance matching.

Group delay measurement is an important antenna parameter as it informs about the degree of distortion between transmitted and received signals and preferably it should be below 0.5ns [9]. Measured and simulated group delay of less than 0.5 ns is observed (cf. Fig. 6b) for the proposed antenna which is desirable.

The radiation mechanism of the proposed antenna can be understood from the observation of simulated current distributions at two resonant frequencies (ie 5.33 GHz (min.)

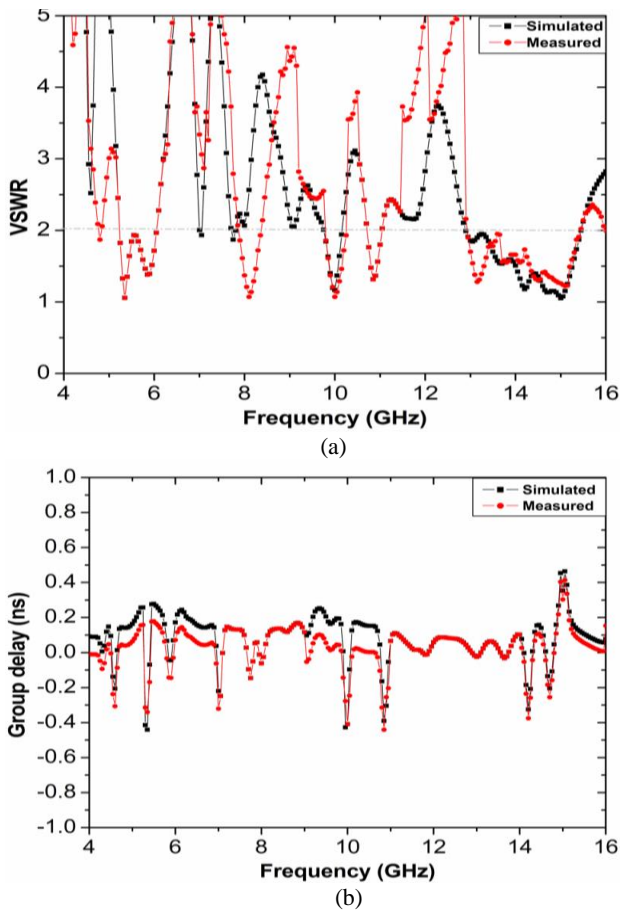


Fig.6. (a) Simulated and measured VSWR as function of frequency of proposed antenna, (b) Simulated and measured group delay as function of frequency of proposed antenna

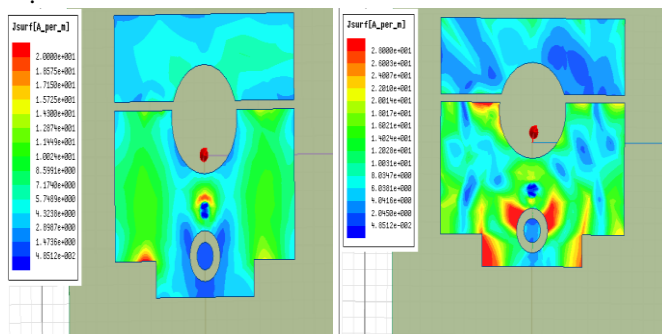


Fig. 7. Current distribution at frequency (a) 5.33GHz (b) 14.3 GHz

and 14.3 GHz (max.) as shown in Fig.7. These resonant frequencies correspond to the lower and higher bands of proposed antenna. The maximum simulated surface current density at 5.33 GHz and 14.3 GHz is 20.02 A/m and 28.08A/m respectively. It has been observed from Fig.7 that current is highly distributed along the edges of the lower patch at both frequencies and is almost equally distributed over the patch. Therefore, this is suggestive that the ground plane surface current is dominantly affecting and controlling the resonance and radiation of antenna. At both frequencies current is mainly distributed on the lower edge of the ground plane, which suggests that the portion of the ground plane close to the patch acts as the part of radiating surface.

The simulated far field radiation pattern (dB) representing co-polarization and cross-polarization components in E plane ($\Phi=0^\circ$) and H-plane ($\Phi=90^\circ$) at frequencies (5.33 GHz, 14.3GHz) are presented in Figs. 8 and 9 respectively. Shape of radiation pattern at resonating frequency is nearly circular. Level of cross polarization is lower than co-polarization at resonant frequencies for both E-plane and H-plane (cf. Fig.8 & 9).

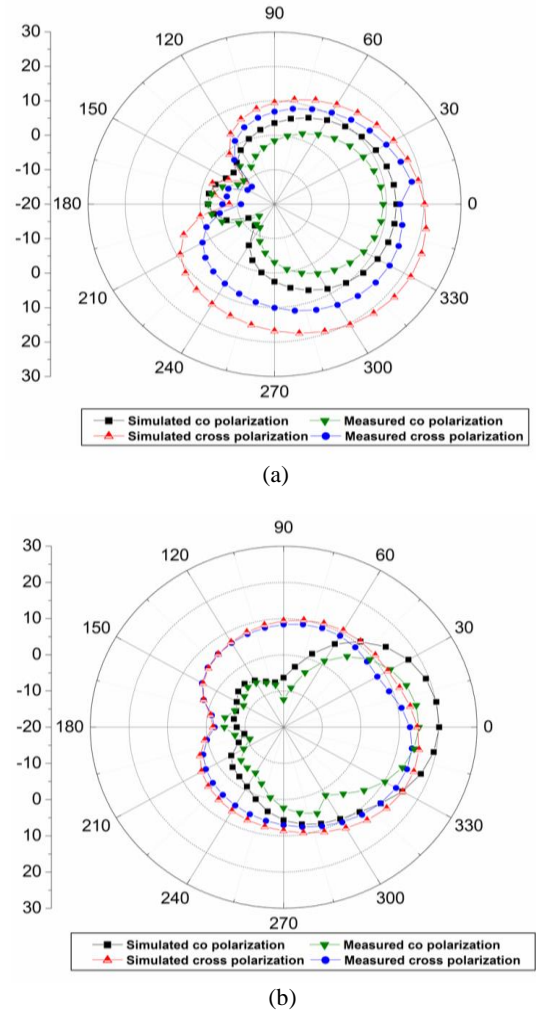
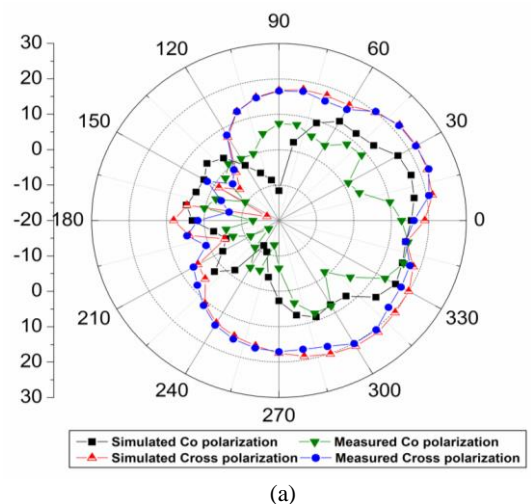


Fig. 8. Radiation pattern of antennas at resonating frequency 5.33 GHz in (a) E plane (b) H plane



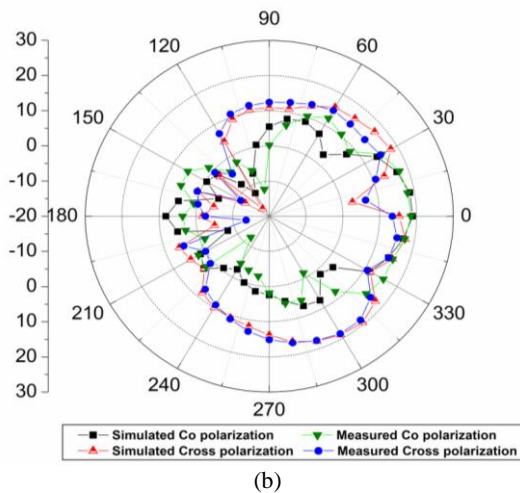


Fig. 9. Radiation pattern of antennas at resonating frequency 14.33 GHz in (a) E plane (b) H plane

IV. CONCLUSION

A new dual band integrated wideband multi resonating patch antenna fed by co-axial probe feed is presented, simulated and experimentally verified for C-band and Ku-band applications. Rectangular patch with circular and linear gap is used for increasing number of bands in band characteristics of antenna. Antenna operation has been explained in terms of return loss, VSWR, gain, radiation pattern and current distribution at different resonating frequencies. The simulated (measured) result cover the frequency band from 5.24-5.95 GHz (5.35-5.9 GHz) and 13.25-15.47 GHz (13.35-15.35 GHz) with maximum gain (simulated) of 3.6dB and 6.0 dB respectively. Good agreement in simulated and measured result with slight deviation is observed. The optimized antenna clearly shows large bandwidth and better return loss.

REFERENCES

- [1] Balanis C. A.(2005), *Antenna Theory: Analysis and Design*. 3rd edition, John Wiley & Sons.
- [2] Garg R., Bahartia P., & Ittipiboon A. (2001), *Microstrip Antenna Design Handbook*, Artech hose, Boston, London.
- [3] Yadav N. P (2016).Triple U-Slot Loaded Defected Ground Plane Antenna for Multiband Operations. *Microwave Optical Technology Letters*, 58, 124–128.
- [4] Rajkumar R.&Kiran K.U.(2016). A Compact Metamaterial Multiband Antenna for WLAN/Wimax /ITU Band Applications. *AEU-International Journal of Electronics and Communications*, 10, 1-6.
- [5] Mehdipour A., Sebak A. R., Trueman CW., & Denidni TA. (2012). Compact Multiband Planar Antenna for 2.4/3.5/5.2/5.8-GHz Wireless Applications. *IEEE Antennas Wireless Propagation Letters*, 11, 144-147.
- [6] Singh V., Mishra B., Dwivedi A.K., & Singh R.(2018). Inverted L-Notch Loaded Hexaband Circular Patch Antenna for X, Ku /K Band Applications. *Microwave and Optical Technology Letters*, 60, 2081-2088.
- [7] Singh V., Mishra B., Tripathi P.N., & Singh R.(2016). A Compact Quad Band Microstrip Antenna for S and C-Band Application. *Microwave and Optical Technology Letters*, 58, 1365-1369.
- [8] Wang H., Huang X.B., & Fang D.G.(2008). A Single Layer Wideband U-Slot Microstrip Patch Antenna Array. *IEEE Antennas Wireless Propagation Letters*, 7, 9–12.
- [9] Khanna P., Sharma A., Shinghal K., & Kumar A.(2016). A Defected Structure Shaped CPW-Fed Wideband Microstrip Antenna for Wireless Applications. *Journal of Engineering*, 4, 1-7.
- [10] Mishra B., Singh V., & Singh R. (2017). Dual and Wide Band Slot Loaded Stacked Microstrip Patch Antenna for WLAN/Wi-MAX Applications. *Microsyst Technol.*, 23, 3467-3475.
- [11] Rao G.S., Kumar S.S., & Pillalamarri R. (2014). Printed Planar Circular Radiating Patch Ultra Wideband Antennas. *Microsyst Technol.*, 21, 2321–2325.
- [12] Chandel R., & Gautam A.K. (2016). Compact MIMO/diversity slot antenna for UWB applications with band-notched characteristic. *Electronics Letter*, 52, 336–338.
- [13] Kamakshi K., Ansari J.A., Singh A., Aneesh M., & Jaiswal A.K.(2015). A Novel Ultra Wideband Toppled Trapezium-Shaped Patch Antenna with Partial Ground Plane. *Microwave and Optical Technology Letters*, 57, 1983–1986.
- [14] Mishra B., Singh V., Singh R.K., Singh N., & Singh R.(2017). A compact UWB patch antenna with defected ground for Ku/K band applications. *Microwave and Optical Technology Letters*, 60, 1-5.
- [15] Khandelwal M.K., Kanaujia BK, Dwari S., Kumar S., & Gautam A.K.(2014). Bandwidth enhancement and Cross-Polarization Suppression in Ultra Wideband Microstrip Antenna with Defected Ground Plane. *Microwave and Optical Technology Letters*, 56, 2141–2146.
- [16] Azadegan R.(2010). A Ku-Band Planar Antenna Array for Mobile Satellite TV Reception with Linear Polarization. *IEEE Trans Antennas Propagation*, 58, 2097–2101.
- [17] Borji A, Busuioc D., & Safavi-Naeini S.(2009). Efficient, Low-Cost Integrated Waveguide-Fed Planar Antenna Array for Ku-Band Applications. *IEEE Antennas Wireless Propagation Letters*, 8, 336– 339.
- [18] Ilham R., & Kurniawan A. (2015). Design and Implementation of Microstrip Antenna Array on Ku-Band for Satellite TV Reception. *IEEE International Telecommunication Networks Applications Conference*, 185–190.
- [19] Park J.H., Choi H.K., & Kim S.H. (2012). Design of Ku-Band Reflectarray Using Hexagonal Patch with Crossed Slots. *Microwave and Optical Technology Letters*, 54 (10), 2383–2387.
- [20] Yu C, Hong W, Kuai Z, & Wang H. (2012). Ku-Band Linearly Polarized Omni-directional Planar Filtenna. *IEEE Antennas Wireless Propagation Letters*, 11, 310–313.
- [21] Islam M. T., Misran N., & Mobashsher A.T.(2010). Compact Dual band Microstrip Antenna for Ku-band Application. *Information Technology journal* 9(2), 354-358.
- [22] Malisuwan S., Sivaraks J., Madan N., & Suriyakrai N. (2014). Design of Microstrip Patch Antenna for Ku-Band Satellite Communication Applications. *International Journal of Computer and Communication Engineering*, 3(6), 413-416.
- [23] Prasad P.C., & Chatteraj N.(2013). Design Of Compact Ku Band Microstrip Antenna for Satellite Communication. *IEEE Int. Conf. Communication Signal Processing*, 196–200.
- [24] Dalli A., Zenkour L., & Bri S. (2012). Comparison of Circular Sector and Rectangular Patch Antenna Arrays in C-Band. *Journal of Electromagnetic Analysis and Applications*, 4 (11), 457-467.
- [25] Bahloul M.S., Abri M., & Bendimerad F. T. (2012). Stacked Printed Antennas Array for C Band Applications. *International Journal of Distributed and Parallel Systems*, 3(3), 275-286.
- [26] Bairami P., & Zavvari M.(2015). Broad Band Circularly Polarized Square Slot Array Antenna with Improved Sequentially Rotated Feed Network for C-Band Application. *International Journal of Microwave and Wireless Technologies*, 9(1), 171–175.
- [27] Slimani A., Bennani S.D., Alami A.E., & Terhzaz J.(2017). Ultra wideband Planar Microstrip Array Antennas for C-Band Aircraft Weather Radar Applications. *Hindawi International Journal of Antennas and Propagation*, 10, 1115-1122.
- [28] Pandey A.K., & Singh R.(2018). Dual Band Gap Coupled Patch Antenna for Wireless Communications. *ECTI Transactions on Electrical Eng., Electronics and Communications*, 16(1), 39-45.